

Revisiting Weak-to-Strong Consistency in Semi-Supervised Semantic Segmentation

Lihe Yang¹ Lei Qi² Litong Feng³ Wayne Zhang³ Yinghuan Shi^{1*}

¹Nanjing University ²Southeast University ³SenseTime Research

<https://github.com/LiheYoung/UniMatch>

Abstract

In this work, we revisit the weak-to-strong consistency framework, popularized by FixMatch from semi-supervised classification, where the prediction of a weakly perturbed image serves as supervision for its strongly perturbed version. Intriguingly, we observe that such a simple pipeline already achieves competitive results against recent advanced works, when transferred to our segmentation scenario. Its success heavily relies on the manual design of strong data augmentations, however, which may be limited and inadequate to explore a broader perturbation space. Motivated by this, we propose an auxiliary feature perturbation stream as a supplement, leading to an expanded perturbation space. On the other, to sufficiently probe original image-level augmentations, we present a dual-stream perturbation technique, enabling two strong views to be simultaneously guided by a common weak view. Consequently, our overall Unified Dual-Stream Perturbations approach (UniMatch) surpasses all existing methods significantly across all evaluation protocols on the Pascal, Cityscapes, and COCO benchmarks. We also demonstrate the superiority of our method in remote sensing interpretation and medical image analysis.

1 Introduction

Semantic segmentation aims to provide pixel-level predictions to images, which can be deemed as a dense classification task and is fundamental to real-world applications, *e.g.*, autonomous driving. Nevertheless, conventional fully-supervised scenario [43, 77, 73] is extremely hungry for delicately labeled images by human annotators, greatly hindering its broad application to some fields where it is costly and even infeasible to annotate abundant images. Therefore, semi-supervised semantic segmentation [56] has been proposed and is attracting increasing attention. Generally, it wishes to alleviate the labor-intensive process via leveraging a large quantity of unlabeled images, accompanied with a handful of manually labeled images.

Following closely the research line of semi-supervised learning (SSL), advanced methods in semi-supervised semantic segmentation have evolved from GANs-based adversarial training paradigm [21, 56, 47] into the widely adopted consistency regularization framework [19, 49, 81, 12, 28, 29, 62] and reborn self-training pipeline [70, 27, 68, 23]. In this work, we focus on the *weak-to-strong* consistency regularization framework, that is popularized by FixMatch [55] from the field of semi-supervised classification, and then impacts many other relevant tasks [41, 57, 66, 45, 63, 67]. The weak-to-strong approach supervises a strongly perturbed unlabeled image x^s with the prediction

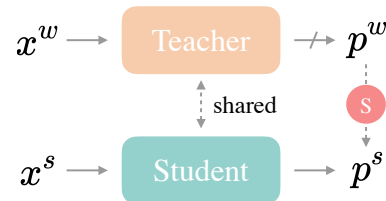


Figure 1: FixMatch. Detached teacher yields pseudo label p^w on weakly perturbed x^w to supervise (S) its strongly perturbed x^s and corresponding prediction p^s . Labeled images are omitted.

*Corresponding author.

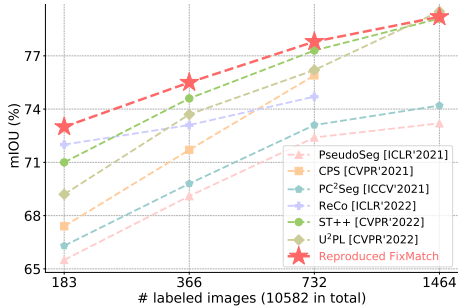


Figure 2: Comparison between current SOTAs and our reproduced FixMatch on the Pascal dataset.

Table 1: The importance of image-level strong perturbations (SP) to FixMatch on the Pascal dataset. *w/o any SP*: directly utilize hard label of x^w to supervise its logits. *w/ CutMix*: only use CutMix [71] as a perturbation, similar to [12]. *w/ whole SP*: strong perturbations contain color transformations from ST++ [68], together with CutMix.

| Method | # labeled images (10582 in total) | | | | |
|-------------|-----------------------------------|-------------|-------------|-------------|-------------|
| | 92 | 183 | 366 | 732 | 1464 |
| w/o any SP | 39.5 | 52.7 | 65.5 | 69.2 | 74.6 |
| w/ CutMix | 56.7 | 67.9 | 71.9 | 75.1 | 78.3 |
| w/ whole SP | 63.9 | 73.0 | 75.5 | 77.8 | 79.2 |

yielded from its corresponding weakly perturbed version x^w , as illustrated in Figure 1. Intuitively, its success lies in that the model is more likely to produce high-quality prediction on x^w , while x^s is more effective for our model to learn, since the strong perturbations introduce additional information as well as mitigate confirmation bias [2]. We surprisingly notice that, so long as coupled with appropriate strong perturbations, FixMatch can indeed still exhibit powerful generalization capability in our scenario, obtaining competitive results against state-of-the-art (SOTA) methods, as compared in Figure 2. Thus, we select this simple yet effective framework as our baseline.

Through investigation on image-level strong perturbations, we observe that they play an indispensable role in making the FixMatch a rather strong competitor in semi-supervised semantic segmentation. As demonstrated in Table 1, the performance gap between whether to adopt perturbations is extremely huge. Greatly inspired by these clues, we hope to inherit the spirit of strong perturbations from FixMatch, but also further strengthen them from two different perspectives and directions, namely *expanding a broader perturbation space*, and *sufficiently harvesting original perturbations*. Each of these two perspectives is detailed in the following two paragraphs respectively.

Image-level perturbations, *e.g.*, color jitter and CutMix [71], include heuristic biases, which actually introduce additional prior information into the bootstrapping paradigm of FixMatch, so as to capture the merits of consistency regularization. In case not equipped with these perturbations, FixMatch will be degenerated to a naive online self-training pipeline, producing much worse results. Despite its effectiveness, these perturbations are totally constrained at the image level, hindering the model to explore a broader perturbation space and to maintain consistency at diverse levels. To this end, in order to expand original perturbation space, we design a unified perturbation framework for both raw images and extracted features. Concretely, on raw images, similar to FixMatch, pre-defined image-level strong perturbations are applied, while for extracted features of weakly perturbed images, an embarrassingly simple channel dropout is inserted. In this way, our model pursues the equivalence of predictions on unlabeled images at both the image and embedding level. These two perturbation levels can be complementary to each other. Distinguished from [33, 42], we separate different levels of perturbations into independent streams to avoid a single stream being excessively hard to learn.

On the other hand, current FixMatch framework merely utilizes a single strong view of each unlabeled image in a mini-batch, which is insufficient to fully exploit the manually pre-defined perturbation space. Considering this, we present a simple yet highly effective improvement to the input, where dual independent strong views are randomly sampled from the perturbation pool. They are then fed into the student model in parallel, and simultaneously supervised by their shared weak view. Such a minor modification even easily turns the FixMatch baseline into a SOTA framework by itself. Intuitively, we conjecture that enforcing two strong views to be close to a common weak view can be regarded as minimizing the distance between these strong views. Hence, it shares the spirits and merits of contrastive learning [11, 25], which can learn more discriminative representations and is proved to be particularly beneficial to our current task [40, 62]. We conduct comprehensive studies on the effectiveness of each proposed component. Our contributions can be summarized in four folds:

- We notice that, coupled with appropriate image-level strong perturbations [71, 68], FixMatch is still a powerful framework when transferred to the semantic segmentation scenario. A plainly reproduced FixMatch outperforms almost all existing methods in current task.
- Built on FixMatch, we propose a unified perturbation approach that unifies image-level and feature-level perturbations in independent streams, to exploit a broader perturbation space.

- We design a dual-stream perturbation strategy to fully probe pre-defined image-level perturbations, as well as to harvest the merits of contrastive learning for discriminative features.
- Our overall framework that integrates above two approaches, dubbed as UniMatch, remarkably surpasses existing methods across all splits on the Pascal, Cityscapes, and COCO. It is also validated in medical image analysis and remote sensing interpretation (Appendix E).

2 Related Work

Semi-supervised learning. The core issue in semi-supervised learning (SSL) lies in how to design reasonable and effective supervision signals for unlabeled data. Two main branches of methodology are proposed to tackle the issue, namely entropy minimization [22, 53, 37, 65, 80, 51] and consistency regularization [36, 54, 58, 64, 30, 6, 5, 48, 20, 38]. Entropy minimization, popularized by self-training [37], works in a straightforward way via assigning pseudo labels to unlabeled data and then combining them with manually labeled data for further re-training. For another thing, consistency regularization holds the assumption that prediction of an unlabeled example should be invariant to different forms of perturbations. Among them, FixMatch [55] proposes to inject strong perturbations to unlabeled images and supervise training process with predictions from weakly perturbed ones to subsume the merits of both methodologies. Recently, FlexMatch [72] and FreeMatch [61] consider learning status of different classes and then filter low-confidence labels with class-wise thresholds. Our method inherits from FixMatch, however, we investigate a more challenging and labor-intensive setting. More importantly, we demonstrate the significance of image-level strong perturbations, thereby managing to expand original perturbation space and take full advantage of pre-defined perturbations.

Semi-supervised semantic segmentation. Earlier works [47, 56] incorporate the GANs [21] as an auxiliary supervision for unlabeled images via discriminating pseudo labels from manual labels. Motivated by the rapid progress in SSL, recent methods [49, 18, 32, 46, 81, 79, 78, 1, 75, 40, 42, 34, 74] strive for simpler training paradigms from the perspective of consistency regularization and entropy minimization. During this trend, French *et al.* [19] disclose Cutout [16] and CutMix [71] are critical to success of consistency regularization in segmentation. AEL [28] then designs an adaptive CutMix and sampling strategy to enhance the learning on under-performing classes. Inspired by contrastive learning, Lai *et al.* [35] propose to enforce predictions of the shared patch under different contextual crops to be same. And U²PL [62] treats uncertain pixels as reliable negative samples to contrast against corresponding positive samples. Similar to the core spirit of co-training [7, 52] and mutual learning [76], CPS [12] introduces dual independent models to supervise each other.

Other works from the research line of entropy minimization utilize a self-training pipeline to assign pseudo masks for unlabeled images in an offline manner. From this perspective, Yuan *et al.* [70] claim excessive perturbations on unlabeled images are catastrophic to clean data distribution, and thus propose a separate batch normalization for these images. Concurrently, ST++ [68] points out that appropriate strong data perturbations are indeed extremely helpful to self-training. Moreover, to tackle the class bias issue encountered in pseudo labeling, He *et al.* [27] align class distributions between manually labeled and pseudo labeled data. And USRN [23] chooses to cluster balanced subclass distributions as a regularization to alleviate the imbalance of pre-defined classes.

To pursue elegance and effectiveness meantime, we adopt the weak-to-strong consistency regularization framework from FixMatch [55], which can be end-to-end trained in a single stage with a single model. Our baseline framework can be deemed as an improvement of [19], or a simplification of [81]. For instance, it strengthens image-level strong perturbations in [19] based on [68], and discards the calibration fusion module in [81]. With this neat and competitive baseline, we further probe a broader perturbation space, and fully exploit original image-level perturbations as well.

3 Method

Provided a relatively small set of labeled images $\mathcal{D}^l = \{(x_i^l, y_i^l)\}$ and a large amount of unlabeled images $\mathcal{D}^u = \{x_i^u\}$, algorithms in semi-supervised semantic segmentation aim to fully explore \mathcal{D}^u with limited amount of annotations from \mathcal{D}^l . Since our method is based on FixMatch [55], we first briefly review its core idea (§3.1). Following this, we introduce the two proposed components in detail, namely unified perturbations (§3.2), as well as dual-stream perturbations (§3.3). Finally, we provide a summary of our overall Unified Dual-Stream Perturbations method (UniMatch) (§3.4).

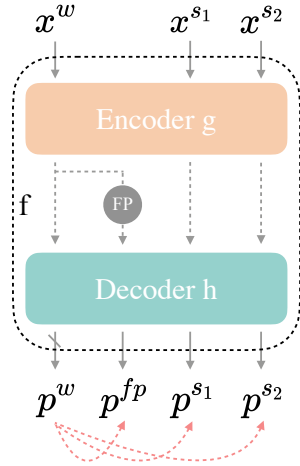


Figure 3: Our proposed unified dual-stream perturbations method (UniMatch). The FP denotes feature perturbation, and the **dashed red curves** represent supervision.

Algorithm 1 Pseudocode of UniMatch in a PyTorch-like style.

```

# f: network, composed of an encoder g and a decoder h
# aug_w/aug_s: weak/strong image-level perturbations

for x in loader_u:
    # one weak view and two strong views as input
    x_w = aug_w(x)
    x_s1, x_s2 = aug_s(x_w), aug_s(x_w)

    # feature of weakly perturbed image
    feat_w = g(x_w)
    # perturbed feature
    feat_fp = nn.Dropout2d(0.5)(feat_w)

    # four predictions (p_w, p_fp, p_s1, p_s2): BxCxHxW
    p_w, p_fp = h(torch.cat((feat_w, feat_fp))).chunk(2)
    p_s1, p_s2 = f(torch.cat((x_s1, x_s2))).chunk(2)

    # hard (one-hot) pseudo mask
    mask_w = p_w.argmax(dim=1).detach()

    # loss from image- and feature-level perturbation
    criterion = nn.CrossEntropyLoss()
    p_s = torch.cat((p_s1, p_s2))
    loss_s = criterion(p_s, mask_w.repeat(2, 1, 1))
    loss_fp = criterion(p_fp, mask_w)

    # final unsupervised loss
    loss_u = (loss_s + loss_fp) / 2.0

```

3.1 Preliminaries

As aforementioned, FixMatch utilizes a weak-to-strong consistency regularization to leverage unlabeled data. Concretely, each unlabeled image x^u is simultaneously perturbed by two operators, *i.e.*, weak perturbation \mathcal{A}^w such as cropping, and strong perturbation \mathcal{A}^s such as color jitter. Then, the overall objective function is a combination of supervised loss \mathcal{L}^s and unsupervised loss \mathcal{L}^u as:

$$\mathcal{L} = \mathcal{L}^s + \sigma \mathcal{L}^u. \quad (1)$$

Typically, the supervised term \mathcal{L}^s is the cross-entropy loss between model predictions and groundtruth labels. And the unsupervised loss \mathcal{L}^u regularizes prediction of the sample under strong perturbations to be the same as that under weak perturbations, which can be formulated as:

$$\mathcal{L}^u = \frac{1}{B_u} \sum \mathbb{1}(\max(p^w) \geq \tau) \mathbb{H}(p^w, p^s), \quad (2)$$

where B_u is batch size of unlabeled images and τ is a pre-defined confidence threshold to filter noisy labels. $\mathbb{H}(p^w, p^s)$ minimizes the entropy between two probability distribution terms, produced by:

$$p^w = \hat{F}(\mathcal{A}^w(x^u)); \quad p^s = F(\mathcal{A}^s(\mathcal{A}^w(x^u))), \quad (3)$$

where the teacher model \hat{F} produces pseudo labels on weakly perturbed images, while the student F leverages strongly perturbed images along with obtained pseudo labels for model optimization. In this work, we set \hat{F} exactly the same as F for simplicity, following FixMatch.

3.2 Unified Image- and Feature-Level Perturbations

Apart from semi-supervised classification, the methodology in FixMatch has swept across a wide range of research topics and achieved booming success, such as semantic segmentation [19, 81, 28], object detection [41, 57, 66], unsupervised domain adaptation [45], and action recognition [63, 67]. Despite its popularity, its efficacy actually heavily depends on delicately designed strong perturbations from researchers, whose optimal combinations and hyper-parameters are time-consuming to acquire. Besides, in some cases such as medical image analysis and remote sensing interpretation, it may require domain-specific knowledge to figure out promising ones. More importantly, these perturbations are completely constrained at the image level, hindering the student model to maintain multi-level consistency against more diverse perturbations.

To this end, in order to construct a broader perturbation space, built on top of FixMatch, we propose to inject perturbations on features of the *weakly* perturbed image x^w . We choose to separate different levels of perturbations into multiple independent feedforward streams, enabling the student to achieve targeted consistency in each stream more directly. Formally, a segmentation model f can be decomposed into an encoder g and a decoder h . In addition to acquired p^w and p^s in FixMatch, we also obtain p^{fp} from an auxiliary feature perturbation stream by:

$$e^w = g(x^w), \quad (4)$$

$$p^{fp} = h(\mathcal{P}(e^w)), \quad (5)$$

where e^w is extracted features of x^w , and \mathcal{P} denotes feature perturbations, *e.g.*, dropout or adding uniform noise.

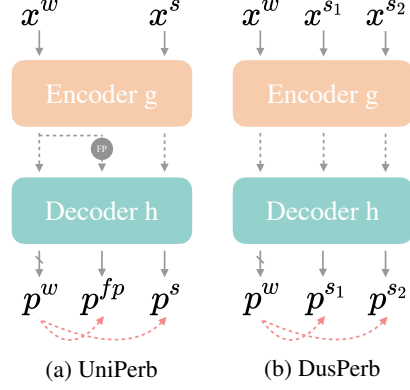


Figure 4: Our UniPerb and DusPerb.

Overall, as exhibited in Figure 4a, three feedforward streams are maintained for each unlabeled mini-batch, which are (i) the simplest stream: $x^w \rightarrow f \rightarrow p^w$, (ii) image-level strong perturbation stream: $x^s \rightarrow f \rightarrow p^s$, and (iii) our introduced feature perturbation stream: $x^w \rightarrow g \rightarrow \mathcal{P} \rightarrow h \rightarrow p^{fp}$. In this way, the student model is enforced to be consistent to unified perturbations at both image and feature level. We name it as UniPerb for convenience. The unsupervised loss \mathcal{L}^u is formulated as:

$$\mathcal{L}^u = \frac{1}{B_u} \sum \mathbb{1}(\max(p^w) \geq \tau) (\mathbb{H}(p^w, p^s) + \mathbb{H}(p^w, p^{fp})). \quad (6)$$

It should be noted that, we do not aim at proposing a novel feature perturbation approach in this work. Actually, an extremely simple Channel Dropout (nn.Dropout2d in PyTorch) is well-performed enough. Furthermore, distinguished from recent work [42] that mixes three levels of perturbations into a single stream, we highlight the necessity of separating perturbations of different properties into independent streams, which is evidenced in our ablation studies. We believe that, image-level perturbations can be well complemented by feature-level perturbations.

3.3 Dual-Stream Perturbations

Motivated by the tremendous advantages of image-level strong perturbations, we wish to fully explore them. We are inspired by recent progress in self-supervised learning and semi-supervised classification, that constructing multiple views for unlabeled data as inputs can better leverage the perturbations. For instance, SwAV [8] proposes a novel technique called `multi-crop`, enforcing the local-to-global consistency among a bag of views of different resolutions. Likewise, ReMixMatch [5] produces multiple strongly augmented versions for the model to learn.

Therefore, we wonder whether such a simple idea can also benefit our semi-supervised semantic segmentation. Similar to ReMixMatch, we make a straightforward attempt that, rather than feeding a single p^s into the model, we independently yield dual-stream perturbations (x^{s1}, x^{s2}) from x^w by strong perturbation pool \mathcal{A}^s . Since \mathcal{A}^s is pre-defined but non-deterministic, x^{s1} and x^{s2} are not equal. Our dual-stream perturbation framework, simply denoted as DusPerb, is displayed in Figure 4b.

Intriguingly, such a minor modification brings consistent and substantial improvements over original FixMatch under all partition protocols in our segmentation scenario, establishing new state-of-the-art results. It is validated in our ablation studies that, the performance gain is non-trivial, not credited to a doubled unlabeled batch size. We conjecture that regularizing two strong views with a shared weak view can be regarded as enforcing consistency between these two strong views as well. Intuitively, suppose k_w is the classifier weight of the class predicted by x^w , and (q_{s1}, q_{s2}) are features of images (x^{s1}, x^{s2}), then in our adopted cross entropy loss, we maximize $q_j \cdot k_w$ against $\sum_{i=0}^C q_j \cdot k_i$, where $j \in \{s1, s2\}$, and k_i is classifier weight of class i . It thus can be deemed that we are also maximizing the similarity between q_{s1} and q_{s2} . Therefore, the InfoNCE loss [59] is satisfied:

$$\mathcal{L}_{s1 \leftrightarrow s2} = -\log \frac{\exp(q_{s1} \cdot q_{s2})}{\sum_{i=0}^C \exp(q_j \cdot k_i)}, \quad s.t., j \in \{s1, s2\}, \quad (7)$$

where q_{s1} and q_{s2} are positive pairs, while all other classifier weights except k_w are negative samples.

Hence, it shares the spirits of contrastive learning [11, 25, 13], which is able to learn more discriminative representations and has been proved to be highly meaningful to current task [40, 62].

Table 2: Comparison with state-of-the-art methods on the **Pascal** dataset with ResNet-101. Labeled images are from the *original high-quality* training set. The fractions (e.g., 1/115) and integers (e.g., 92) denote the proportion and number of labeled images respectively. †: Their training size is larger than us: 512 vs. 321.

| Method | 1/115 (92) | 1/57 (183) | 1/28 (366) | 1/14 (732) | 1/7 (1464) |
|------------------------------------|-------------|-------------|-------------|-------------|-------------|
| Supervised Baseline | 45.1 | 55.3 | 64.8 | 69.7 | 73.5 |
| CutMix-Seg [19] [BMVC'20] | 52.2 | 63.5 | 69.5 | 73.7 | 76.5 |
| PseudoSeg [81] [ICLR'21] | 57.6 | 65.5 | 69.1 | 72.4 | 73.2 |
| PC ² Seg [78] [ICCV'21] | 57.0 | 66.3 | 69.8 | 73.1 | 74.2 |
| CPS† [12] [CVPR'21] | 64.1 | 67.4 | 71.7 | 75.9 | - |
| ReCo [40] [ICLR'22] | 64.8 | 72.0 | 73.1 | 74.7 | - |
| ST++ [68] [CVPR'22] | 65.2 | 71.0 | 74.6 | 77.3 | 79.1 |
| U ² PL† [62] [CVPR'22] | 68.0 | 69.2 | 73.7 | 76.2 | 79.5 |
| PS-MT† [42] [CVPR'22] | 65.8 | 69.6 | 76.6 | 78.4 | 80.0 |
| UniMatch [Ours] | 75.2 | 77.2 | 78.8 | 79.9 | 81.2 |

Table 3: Comparison with state-of-the-art methods on the **Pascal** dataset. Labeled images are sampled from the *blended* training set, which is augmented by the SBD dataset. ‡: We reproduce its ResNet-50 results.

| Method | Training Size | ResNet-50 | | | ResNet-101 | | |
|-----------------------------------|---------------|-------------|-------------|-------------|-------------|-------------|-------------|
| | | 1/16 (662) | 1/8 (1323) | 1/4 (2646) | 1/16 (662) | 1/8 (1323) | 1/4 (2646) |
| Supervised Baseline | 321×321 | 61.2 | 67.3 | 70.8 | 65.6 | 70.4 | 72.8 |
| CAC [35] [CVPR'21] | 320×320 | 70.1 | 72.4 | 74.0 | 72.4 | 74.6 | 76.3 |
| ST++ [68] [CVPR'22] | 321×321 | 72.6 | 74.4 | 75.4 | 74.5 | 76.3 | 76.6 |
| UniMatch [Ours] | 321×321 | 74.5 | 75.8 | 76.1 | 76.5 | 77.0 | 77.2 |
| Supervised Baseline | 513×513 | 62.4 | 68.2 | 72.3 | 67.5 | 71.1 | 74.2 |
| CutMix-Seg [19] [BMVC'20] | 512×512 | 68.9 | 70.7 | 72.5 | 72.6 | 72.7 | 74.3 |
| CPS [12] [CVPR'21] | 512×512 | 72.0 | 73.7 | 74.9 | 74.5 | 76.4 | 77.7 |
| ELN [34] [CVPR'22] | 512×512 | - | 73.2 | 74.6 | - | 75.1 | 76.6 |
| U ² PL‡ [62] [CVPR'22] | 513×513 | 72.0 | 75.1 | 76.2 | 74.4 | 77.6 | 78.7 |
| PS-MT [42] [CVPR'22] | 512×512 | 72.8 | 75.7 | 76.4 | 75.5 | 78.2 | 78.7 |
| UniMatch [Ours] | 513×513 | 75.8 | 76.9 | 76.8 | 78.1 | 78.4 | 79.2 |

3.4 Our Holistic Framework: Unified Dual-Stream Perturbations (UniMatch)

To sum up, we present two key techniques to leverage unlabeled images, namely UniPerb and DusPerb. Our holistic framework (dubbed as UniMatch) that integrates both approaches is illustrated in Figure 3. The corresponding pseudocode is provided in Algorithm 1. In comparison with FixMatch, two auxiliary feedforward streams are maintained, one for perturbation on features of x^w , and the other for multi-view learning of (x^{s1}, x^{s2}) . The final unsupervised term is computed as:

$$\mathcal{L}^u = \frac{1}{B_u} \sum \mathbb{1}(\max(p^w) \geq \tau) (\lambda \text{H}(p^w, p^{fp}) + \frac{\mu}{2} (\text{H}(p^w, p^{s1}) + \text{H}(p^w, p^{s2}))). \quad (8)$$

It is clarified that feature perturbation stream and image-level perturbation stream have their own properties and advantages, thus their loss weights λ and μ are equally set as 0.5. The weight term σ of \mathcal{L}^u is set as 1, also same as that of \mathcal{L}^s . The objective function H in \mathcal{L}^u is a regular cross entropy loss. Following FixMatch, the confidence threshold τ is set as 0.95 in all our experiments.

4 Experiments

In this section, we first provide some implementation details of our whole framework (§4.1). Then in order to better demonstrate the superiority of our proposed UniMatch, we perform thorough comparisons with previous state-of-the-art (SOTA) methods on the Pascal, Cityscapes, and COCO benchmarks (§4.2). More importantly, we conduct extensive ablation studies on the effectiveness of each single component, as well as its simple alternatives (§4.3).

Table 4: Comparison with state-of-the-art methods on the **Cityscapes** dataset. ‡: Reproduced on RN-50.

| Method | ResNet-50 | | | Method | ResNet-101 | | |
|------------------------------------|---------------|--------------|--------------|----------------------------------|---------------|--------------|--------------|
| | 1/30 (100) | 1/8 (372) | 1/4 (744) | | 1/16 (186) | 1/8 (372) | 1/4 (744) |
| SupBaseline | 56.8 | 70.8 | 73.7 | SupBaseline | 67.9 | 73.5 | 75.4 |
| CAC [35] [CVPR'21] | - | 69.7 | 72.7 | CutMix-Seg [BMVC'20] | 67.1 | 71.8 | 76.4 |
| PC ² Seg [78] [ICCV'21] | 60.4 | 72.1 | 73.8 | CPS [12] [CVPR'21] | 69.8 | 74.3 | 74.6 |
| ELN [34] [CVPR'22] | - | 70.3 | 73.5 | AEL [28] [NeurIPS'21] | 74.5 | 75.6 | 77.6 |
| ST++ [68] [CVPR'22] | 61.4 | 72.7 | 73.8 | PS-MT [42] [CVPR'22] | - | 76.9 | 77.6 |
| U ² PL ‡ [62] [CVPR'22] | 59.8 | 73.0 | 76.3 | U ² PL [62] [CVPR'22] | 74.9 | 76.5 | 78.5 |
| UniMatch [Ours] | 64.5 | 75.6 | 77.4 | UniMatch [Ours] | 75.7 | 77.3 | 78.7 |

Table 5: Comparisons with state-of-the-art methods on the **COCO** dataset with Xception-65 backbone.

| Method | 1/512 (232) | 1/256 (463) | 1/128 (925) | 1/64 (1849) | 1/32 (3697) |
|------------------------------------|-------------|-------------|-------------|-------------|-------------|
| Supervised Baseline | 22.9 | 28.0 | 33.6 | 37.8 | 42.2 |
| PseudoSeg [81] [ICLR'21] | 29.8 | 37.1 | 39.1 | 41.8 | 43.6 |
| PC ² Seg [78] [ICCV'21] | 29.9 | 37.5 | 40.1 | 43.7 | 46.1 |
| UniMatch [Ours] | 32.2 | 40.4 | 46.2 | 48.7 | 51.2 |

4.1 Implementation Details

For fair comparison with prior works, we mainly adopt DeepLabv3+ [10] based on ResNet [26] as our segmentation model. During training, each mini-batch is composed of both labeled images and unlabeled images, whose quantity is the same, both 8 in all datasets. The initial learning rate is set as 0.001, 0.005, and 0.004 for Pascal, Cityscapes, and COCO respectively, with a SGD optimizer. The model is trained for 80, 240, and 30 epochs under a poly learning rate scheduler. We borrow exactly the same image-level strong perturbations \mathcal{A}^s from ST++ [68], except replacing its Cutout [16] with CutMix [71]. The weakly perturbed image x^w is randomly cropped, flipped, and resized between 0.5 and 2.0 from raw image. The training crop size is set as 321, 769, and 513 for these three datasets. By default, we adopt a channel dropout of 50% probability (`nn.Dropout2d(0.5)` in PyTorch) as our feature perturbation, which is inserted at the intersection of encoder and decoder.

4.2 Comparison with State-of-the-Art Methods

Pascal VOC 2012. The Pascal dataset [17] is originally constructed of 1464 high-quality training images and 1449 validation images. Later, it is expanded by extra relatively coarse manual annotations from the SBD dataset [24], resulting in a total of 10582 training images. Following prior arts, we randomly select labeled images from 1) the original high-quality training images, and 2) the blended 10582 training images. On the first data partition criterion, which we believe is more convincing, our UniMatch outperforms existing methods tremendously, as indicated in Table 2. Especially on the scarce-label regimes, such as only 92 and 183 labeled images available, our method is superior to previous best results by 9.2% and 5.2% respectively. It is also worth noting that, our method adopts a smaller training size of 321 than most recent works of 512, which makes ours more efficient to train. In addition, on the second partition where labeled images are from the blended set, we compare our UniMatch with previous methods at different training resolutions of 321 and 513. As demonstrated in Table 3, our method still gains remarkable improvements over up-to-date works.

Cityscapes. The Cityscapes dataset [15], focusing on urban scenes, consists of 2975 high-resolution training images and 500 validation images. We follow experimental details of U²PL [62], such as performing sliding window evaluation and replacing cross entropy loss in \mathcal{L}^s with a better online hard example mining loss. We report results under both the ResNet-50 and ResNet-101 backbone, and make a comparison with U²PL in Table 4. Our performance is consistently better than that of U²PL.

MS COCO. The COCO dataset [39], composed of 118k/5k training/validation images, is a quite challenging benchmark for semantic segmentation, containing 81 classes to predict. Therefore, it was rarely explored before in semi-supervised works of segmentation. However, in view of the seemingly saturate performance on the Pascal and Cityscapes, we believe it will be more practical to evaluate our

Table 6: Effectiveness of each proposed component under different data partitions and backbones. *: We borrow previous SOTA results from Table 2 and 3, that are obtained with the same size (321) as us. We compare our reproduced FixMatch with previous SOTAs, and the better results are underlined.

| Method | ResNet-101 | | | | | ResNet-50 | | | ResNet-101 | | |
|---------------------|-------------|-------------|-------------|-------------|-------------|-------------|-------------|-------------|-------------|-------------|-------------|
| | 92 | 183 | 366 | 732 | 1464 | 1/16 | 1/8 | 1/4 | 1/16 | 1/8 | 1/4 |
| SOTA Before* | <u>65.2</u> | 72.0 | 74.6 | 77.3 | 79.1 | 72.6 | 74.4 | 75.4 | 74.5 | 76.3 | 76.6 |
| FixMatch (Figure 1) | 63.9 | <u>73.0</u> | <u>75.5</u> | <u>77.8</u> | <u>79.2</u> | <u>73.6</u> | 73.4 | 74.2 | 74.1 | 75.9 | 76.4 |
| UniPerb (Figure 4a) | 72.0 | 75.8 | 77.5 | 79.3 | 80.1 | 74.2 | 74.8 | 75.1 | 76.0 | 76.9 | 76.6 |
| DusPerb (Figure 4b) | 72.1 | 75.9 | 78.3 | 78.1 | 79.6 | 73.8 | 75.1 | 75.4 | 75.3 | 76.5 | 76.6 |
| UniMatch (Figure 3) | 75.2 | 77.2 | 78.8 | 79.9 | 81.2 | 74.5 | 75.8 | 76.1 | 76.5 | 77.0 | 77.2 |

Table 7: Ablation study on the non-trivial improvement of diverse perturbations. Our UniMatch is consistently superior to its counterpart which directly uses triple strongly perturbed images as inputs.

| Method | ResNet-101 | | | | | ResNet-50 | | | ResNet-101 | | |
|--------------------|-------------|-------------|-------------|-------------|-------------|-------------|-------------|-------------|-------------|-------------|-------------|
| | 92 | 183 | 366 | 732 | 1464 | 1/16 | 1/8 | 1/4 | 1/16 | 1/8 | 1/4 |
| Dual Image Views | 72.1 | 75.9 | 78.3 | 78.1 | 79.6 | 73.8 | 75.1 | 75.4 | 75.3 | 76.5 | 76.6 |
| Triple Image Views | 71.6 | 76.4 | 78.4 | 78.8 | 79.6 | 74.1 | 74.7 | 75.7 | 75.4 | 76.1 | 76.8 |
| UniMatch | 75.2 | 77.2 | 78.8 | 79.9 | 81.2 | 74.5 | 75.8 | 76.1 | 76.5 | 77.0 | 77.2 |

algorithms on this dataset. We adopt exactly the same partition protocol and backbone (Xception-65 [14]) as PseudoSeg [81]. As evidenced by Table 5, our UniMatch significantly surpasses all available methods by 2.3%-6.1%, which is much larger than the gap achieved by PC²Seg [78] over PseudoSeg.

4.3 Ablation Studies

Since training on the Cityscapes and COCO dataset is resource-intensive and very time-consuming, we mainly conduct ablation studies on the Pascal dataset across extensive partition protocols.

Individual effectiveness of UniPerb and DusPerb. We promote the perturbation spirit in FixMatch from two different perspectives, and accordingly present two modifications, *i.e.*, UniPerb and DusPerb. Therefore, we need to examine their individual effect. As shown in Table 6, we first demonstrate that our reproduced FixMatch is a strong competitor against previous SOTA methods. Then built upon FixMatch, both UniPerb and DusPerb facilitate their baseline by a large margin. Take 92 labeled images as an example, they improve original FixMatch from 63.9% to 72.0% and 72.1% respectively. Lastly, our overall framework UniMatch that integrates both components obtains the best results.

The improvement of diverse perturbations is non-trivial. Since UniMatch utilizes three views, *i.e.*, one feature perturbation view and dual image perturbation views, to train the student model, we wish to validate that constructing diverse perturbations is beneficial, much better than blindly maintaining three parallel image perturbations. As displayed in Table 7, we compare our UniMatch with a simple counterpart that adopts three image-level strong perturbation views during training. It can be seen that our UniMatch is consistently superior to it, indicating that the improvement brought by UniMatch is not credited to blindly increasing views, but the diversity counts.

The improvement of dual-stream perturbation is non-trivial. Our DusPerb outperforms its FixMatch baseline consistently. However, it might have been noticed that in our DusPerb, the number of unlabeled images in each minibatch is doubled, since each image is strongly perturbed twice. Hence it might be argued that the improvement from DusPerb is due to larger batch size. Considering this concern, we further carry out an ablation study on the FixMatch with a twice larger batch size for unlabeled images under the same training iterations. As presented in Table 8, although increasing the unlabeled batch size ($2 \times$ BS) or lengthening training epochs ($2 \times$ EP) improves the FixMatch baseline in most cases, they are still evidently lagging behind our DusPerb.

The necessity of separating image- and feature-level perturbations into independent streams. PS-MT [42] mixes three levels of perturbations into a single feedforward stream, however, we claim that separating perturbations with different properties into independent streams will enable the model to achieve the targeted invariance more directly, and also avoid single stream being excessively hard.

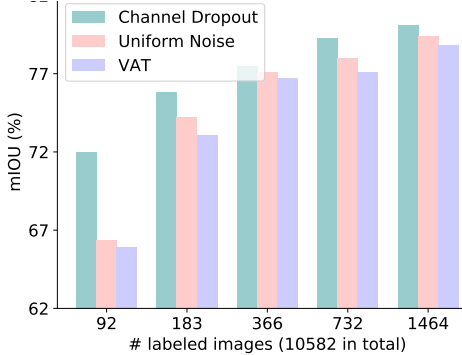


Figure 5: Ablation study on the efficacy of various feature perturbation strategies in our UniPerb method.

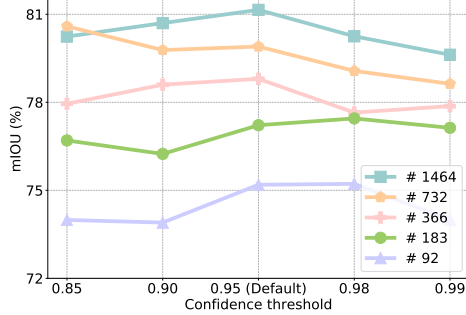


Figure 6: Ablation study on different values of confidence threshold in our UniMatch method. Numbers in the legend denote the number of labeled images.

Table 8: Ablation study on the superiority of dual-stream perturbations over $2\times$ batch size or epochs.

| Method | 92 | 183 | 366 | 732 | 1464 |
|--------------|-------------|-------------|-------------|-------------|-------------|
| $2\times$ BS | 62.5 | 74.5 | 77.1 | 77.8 | 79.3 |
| $2\times$ EP | 61.8 | 73.6 | 76.2 | 77.6 | 79.4 |
| DusPerb | 72.1 | 75.9 | 78.3 | 78.1 | 79.6 |

Table 9: Ablation study on separating image- and feature-level perturbations into independent streams.

| Method | 92 | 183 | 366 | 732 | 1464 |
|----------------|-------------|-------------|-------------|-------------|-------------|
| FixMatch | 63.9 | 73.0 | 75.5 | 77.8 | 79.2 |
| 1 Hybrid View | 63.4 | 72.8 | 75.0 | 76.9 | 78.7 |
| 2 Hybrid Views | 71.8 | 74.6 | 76.8 | 78.4 | 79.6 |
| UniPerb | 72.0 | 75.8 | 77.5 | 79.3 | 80.1 |

To confirm our hypothesis, we inject our dropout perturbation on the features of *strongly* perturbed images, forming a stream of hybrid view. As shown in Table 9, one hybrid view is somewhat inferior to one image perturbation view from FixMatch, indicating this hybrid stream might be too hard to learn generalizable knowledge. Moreover, we attempt to adopt two hybrid views, but observing that it is still worse than our separate practice in UniPerb.

Other feature perturbation strategies. We adopt a simplest form of feature perturbation in our main experiments, which is a channel dropout. There are some other options available, such as uniform noise and virtual adversarial training (VAT) [48]. We follow [49] to set the hyper-parameters in these strategies. And all these options are compared in Figure 5. It can be concluded that a channel dropout performs best.

Table 10: Ablation study on the location to insert feature perturbations in our UniPerb method.

| Location | 92 | 183 | 366 | 732 | 1464 |
|------------|-------------|-------------|-------------|-------------|-------------|
| En-Decoder | 72.0 | 75.8 | 77.5 | 79.3 | 80.1 |
| Classifier | 64.5 | 72.2 | 76.9 | 77.9 | 79.5 |

Value of the confidence threshold τ . Ever since FixMatch, it has been a common practice to set the confidence threshold τ as 0.95 in most datasets to pick out certain samples. We use this default value in all our experiments, but also report the performance of different values in Figure 6. We find that a 0.95 value is still most reliable, but other reasonable values are also acceptable.

Locations to insert feature perturbations. As aforementioned, feature perturbations are injected at the intersection of encoder and decoder in our segmentation model. Previous work [49] also performs perturbations to the input of final classifier. We compare these two perturbation locations in Table 10. It is observed that perturbing features at the intersection of encoder and decoder is much better.

5 Conclusion

In this work, we investigate the promising role of FixMatch in semi-supervised semantic segmentation. We first present that a vanilla FixMatch can indeed perform on par with recent state-of-the-art works, as long as equipped with proper image-level strong perturbations. Inspired by this, we inherit the spirit from FixMatch, but also strengthen its perturbation practice from two different perspectives. On one hand, we propose UniPerb that unifies image- and feature-level perturbations, to form a more diverse perturbation space. On the other, we design a dual-stream perturbation (DusPerb) technique to fully exploit original manually pre-defined perturbations. Both methods facilitate our FixMatch baseline significantly, and our overall integrated method UniMatch achieves remarkable improvement over previous best results on all the Pascal, Cityscapes, and COCO benchmarks.

A Comparison between our UniMatch and FixMatch on the COCO Dataset

As demonstrated in our main paper, our UniMatch has achieved remarkable improvement against the only two methods [81, 78] that provide results on the challenging COCO dataset. Here, we further examine the superiority of our UniMatch compared with its FixMatch baseline [55]. It is evidenced in Table 11 that, our UniMatch boosts the FixMatch significantly across extensive data partition protocols, and the performance gap can be as large as **8.5%** under the 1/128 labeled data setting.

Table 11: Comparisons between our UniMatch and its FixMatch baseline on COCO. We also list the results from PseudoSeg [81] and PC²Seg [78] as a reference. †: The FixMatch is reproduced by us in segmentation scenario.

| Method | 1/512 (232) | 1/256 (463) | 1/128 (925) | 1/64 (1849) | 1/32 (3697) |
|------------------------------------|--------------------|--------------------|--------------------|--------------------|--------------------|
| Supervised Baseline | 22.9 | 28.0 | 33.6 | 37.8 | 42.2 |
| PseudoSeg [81] [ICLR'21] | 29.8 | 37.1 | 39.1 | 41.8 | 43.6 |
| PC ² Seg [78] [ICCV'21] | 29.9 | 37.5 | 40.1 | 43.7 | 46.1 |
| FixMatch† [55] [NeurIPS'20] | 26.8 | 32.8 | 37.7 | 44.1 | 47.5 |
| UniMatch [Ours] | 32.2 (+5.4) | 40.4 (+7.6) | 46.2 (+8.5) | 48.7 (+4.6) | 51.2 (+3.7) |

B How about Removing Image-Level Strong Perturbations?

It has almost become a primary concern and a common practice in various semi-supervised settings to seek for proper image-level strong perturbations first. Nevertheless, this process requires many time-consuming trials and delicate selection of different combinations. To make matters worse, in some domain-specific tasks, such as medical image analysis, it is challenging for most practitioners to figure out appropriate ones. Therefore, a natural question raises: could we replace image-level strong perturbations in FixMatch with a simple channel dropout perturbation at the feature level?

Table 12: Results of only using *single* perturbation level, either image-level perturbations (original FixMatch) or feature-level perturbations. These results are obtained from the Pascal dataset with DeepLabv3+ and ResNet-101. We also provide results of unified levels (our UniPerb) as a reference.

| Perturbation Level | 92 | 183 | 366 | 732 | 1464 | 1/16 | 1/8 | 1/4 |
|------------------------------|------|------|------|------|------|------|------|------|
| Image Level (FixMatch) | 63.9 | 73.0 | 75.5 | 77.8 | 79.2 | 74.1 | 75.9 | 76.4 |
| Feature Level Alone | 66.0 | 69.6 | 74.0 | 77.3 | 78.9 | 73.7 | 74.5 | 76.4 |
| Unified Levels (our UniPerb) | 72.0 | 75.8 | 77.5 | 79.3 | 80.1 | 76.0 | 76.9 | 76.6 |

To validate this, we make a modification to original FixMatch that, input images are not processed by any strong data augmentation, but their features are perturbed by a channel dropout. It can be observed from Table 12 that in most cases, feature-level perturbation alone can indeed perform on par with original image-level strong perturbations in FixMatch, merely slightly inferior. Hence, we believe that such simple but universal feature perturbations may serve as a promising supplement, when image-level strong perturbations fail to work in some rarely explored scenarios.

C Dual-Stream Feature-Level Perturbations

Table 13: Effectiveness of dual-stream perturbations at the feature level. FP here denotes feature perturbation. The dual-stream FP also contains one stream for image-level strong perturbations.

| Method | 92 | 183 | 366 | 732 | 1464 | 1/16 | 1/8 | 1/4 |
|----------------------------|-------------|-------------|-------------|-------------|-------------|-------------|-------------|-------------|
| Single-Stream FP (UniPerb) | 72.0 | 75.8 | 77.5 | 79.3 | 80.1 | 76.0 | 76.9 | 76.6 |
| Dual-Stream FP | 73.4 | 77.1 | 78.5 | 79.6 | 80.4 | 76.2 | 77.0 | 76.8 |

The technique of dual-stream perturbations has been proved to be highly beneficial at the image level. Certainly, we wish to check its effectiveness at the feature level. Thus, we attempt to strengthen our proposed UniPerb via performing twice parallel channel dropout on the extracted features. The dual perturbed features are then sent into the decoder to produce two final predictions for learning. The

results of dual-stream feature-level perturbations are reported in Table 13. Our UniPerb can be further boosted via maintaining dual feature perturbation streams. As discussed in Section 3.3 of our main paper, we conjecture that dual random perturbations on the same features can also be considered to produce a pair of positive views, thereby harvesting the merits of contrastive learning. We decide not to conduct dual-stream feature perturbations in our main approach, since our current UniMatch is powerful enough, and we manage to avoid additional computational burden during training.

D More Perturbation Streams

Motivated by the effectiveness of dual image-level strong streams as well as an auxiliary feature-level stream, we further examine the performance change with respect to the number of these auxiliary image- or feature-level perturbation streams.

D.1 Image-Level Streams Alone

First, the auxiliary feature-level stream is excluded, which means the perturbation space is completely constrained at the image level. Then, we progressively increase the number of image-level strong perturbation streams on the Pascal, and report the corresponding performance in Table 14.

Table 14: The performance change with respect to the number of image-level strong perturbation streams.

| Number of labeled images | Number of image-level perturbation streams | | | | | | |
|--------------------------|--|-------------|------|------|-------------|-------------|------|
| | 1 (FixMatch) | 2 (DusPerb) | 3 | 4 | 5 | 6 | 7 |
| High-quality set: 732 | 77.8 | 78.1 | 78.8 | 78.9 | 79.1 | 78.7 | 78.4 |
| Blended set: 662 (1/16) | 74.1 | 75.3 | 75.4 | 76.1 | 76.0 | 76.7 | 76.3 |

The performance is steadily improved as the number of strong views is increased to a certain number. But if we continue to increase beyond it, then the performance might drop a little. The results indicate that, two or three strong views are already enough to fully probe the original image-level perturbation space. Excessive strong views might cause the model to struggle in learning every single view.

D.2 Image-Level and Feature-Level Streams Together

We also attempt to simultaneously increase the number of image- and feature-level perturbation streams in Table 15. It is observed that, increasing more perturbation streams than our UniMatch does not necessarily result in higher performance. This also indicates that, the two image streams and one feature stream in our UniMatch are well-performed enough.

Table 15: The performance change with respect to the number of image- and feature-level perturbation streams. **IS** is short for image-level stream, while **FS** represents feature-level stream. The first row (IS:2, FS:1) is our UniMatch approach.

| IS | FS | 92 | 183 | 366 | 732 | 1464 | 1/16 | 1/8 | 1/4 |
|----|----|-------------|-------------|-------------|-------------|-------------|-------------|-------------|-------------|
| 2 | 1 | 75.2 | 77.2 | 78.8 | 79.9 | 81.2 | 76.5 | 77.0 | 77.2 |
| 2 | 2 | 75.2 | 77.7 | 78.9 | 79.7 | 80.7 | 76.9 | 77.3 | 77.9 |
| 3 | 3 | 75.5 | 77.0 | 78.6 | 79.5 | 80.5 | 76.7 | 77.7 | 77.3 |
| 4 | 4 | 75.0 | 76.6 | 79.4 | 79.8 | 80.6 | 76.6 | 77.1 | 77.5 |

E Application of our UniMatch to More Segmentation Scenarios

We have validated the efficacy of our UniMatch in common semi-supervised semantic segmentation benchmarks, *i.e.*, the Pascal, Cityscapes, and COCO. However, considering the original motivation of semi-supervised setting, which is to alleviate the annotation burden in real worlds, we carry out extra experiments in two highly practical and critical scenarios, *i.e.*, remote sensing interpretation and medical image analysis. Both scenarios have two distinct characteristics, that raw unlabeled data is relatively easy and cheap to acquire, while manual annotations are labor-intensive and rather costly.

E.1 Remote Sensing Interpretation

Table 16: Comparison with state-of-the-art methods on the **WHU-CD** dataset [31]. The fraction (*e.g.*, 5%) denotes the proportion of labeled images. IOU^c denotes *changed-class IOU*, while OA represents *overall accuracy*.

| Method | 5% | | 10% | | 20% | | 40% | |
|-----------------|----------------|--------------|----------------|--------------|----------------|--------------|----------------|--------------|
| | IOU^c | OA | IOU^c | OA | IOU^c | OA | IOU^c | OA |
| SupBaseline | 50.0 | 97.48 | 55.7 | 97.53 | 65.4 | 98.20 | 76.1 | 98.94 |
| Advent [60] | 55.1 | 97.90 | 61.6 | 98.11 | 73.8 | 98.80 | 76.6 | 98.94 |
| S4GAN [47] | 18.3 | 96.69 | 62.6 | 98.15 | 70.8 | 98.60 | 76.4 | 98.96 |
| SemiCDNet [50] | 51.7 | 97.71 | 62.0 | 98.16 | 66.7 | 98.28 | 75.9 | 98.93 |
| SemiCD [3] | 65.8 | 98.37 | 68.1 | 98.47 | 74.8 | 98.84 | 77.2 | 98.96 |
| UniMatch (Ours) | 77.5 | 99.03 | 79.9 | 99.13 | 82.6 | 99.23 | 86.5 | 99.43 |

We mainly focus on the change detection task in the scenario of remote sensing interpretation, due to its wide application demand and strict labeling requirement. Concretely, given a pair of bi-temporal images, *i.e.*, two images for the same region but of different times, algorithms in change detection are required to discriminate changed regions from unchanged ones by comparing the pair. This task can be simply deemed as a binary segmentation problem, except the minor difference that features of two bi-temporal images extracted by a siamese network will be subtracted first and then fed into the decoder. A demo for this task is illustrated in Figure 7. Following the latest work [3], we validate our UniMatch on two widely acknowledged benchmarks, *i.e.*, WHU-CD [31] and LEVIR-CD [9]. According to the results in Table 16 and Table 17, our method outperforms the recently proposed method [3] impressively. For instance, under the settings of 5% and 10% labeled images, our UniMatch improves previous best IOU^c from 65.8% to 77.5% (+11.7%) and 68.1% to 79.9% (+11.8%), respectively.

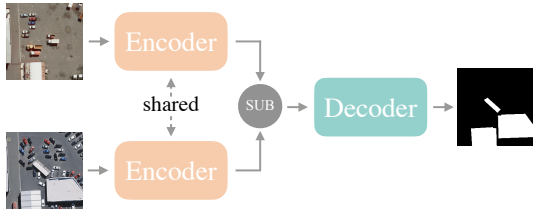


Figure 7: A typical pipeline in change detection task.

Following the latest work [3], we validate our UniMatch on two widely acknowledged benchmarks, *i.e.*, WHU-CD [31] and LEVIR-CD [9]. According to the results in Table 16 and Table 17, our method outperforms the recently proposed method [3] impressively. For instance, under the settings of 5% and 10% labeled images, our UniMatch improves previous best IOU^c from 65.8% to 77.5% (+11.7%) and 68.1% to 79.9% (+11.8%), respectively.

Table 17: Comparison with state-of-the-art methods on the **LEVIR-CD** dataset [9].

| Method | 5% | | 10% | | 20% | | 40% | |
|-----------------|----------------|--------------|----------------|--------------|----------------|--------------|----------------|--------------|
| | IOU^c | OA | IOU^c | OA | IOU^c | OA | IOU^c | OA |
| SupBaseline | 61.0 | 97.60 | 66.8 | 98.13 | 72.3 | 98.44 | 74.9 | 98.60 |
| Advent [60] | 66.1 | 98.08 | 72.3 | 98.45 | 74.6 | 98.58 | 75.0 | 98.60 |
| S4GAN [47] | 64.0 | 97.89 | 67.0 | 98.11 | 73.4 | 98.51 | 75.4 | 98.62 |
| SemiCDNet [50] | 67.6 | 98.17 | 71.5 | 98.42 | 74.3 | 98.58 | 75.5 | 98.63 |
| SemiCD [3] | 72.5 | 98.47 | 75.5 | 98.63 | 76.2 | 98.68 | 77.2 | 98.72 |
| UniMatch (Ours) | 79.0 | 98.86 | 79.3 | 98.89 | 80.1 | 98.92 | 80.5 | 98.93 |

E.2 Medical Image Analysis

We further employ our method to the area of medical image segmentation, which acts as a fundamental role in assisting specialists to diagnosis as well as localize targeted organs or lesions. We follow the latest work [44] to investigate semi-supervised medical segmentation on the ACDC dataset [4]. As shown in Table 18, our UniMatch is superior to existing methods by a tremendous margin, *e.g.*, +21.9% given 3 labeled cases. Our result of mere 1 labeled case even surpasses others with 3 cases, and is on par with others with 7 cases.

Table 18: Comparison with state-of-the-art methods on ACDC [4]. 70 training cases in total. The results are measured by DSC metric averaged on 3 classes.

| Method | 1 case | 3 cases | 7 cases |
|------------------|-------------|-------------|-------------|
| UA-MT [69] | N/A | 61.0 | 81.5 |
| CCT [49] | N/A | 58.6 | 81.6 |
| CPS [12] | N/A | 60.3 | 83.3 |
| CNN & Trans [44] | N/A | 65.6 | 86.4 |
| UniMatch (Ours) | 85.2 | 87.5 | 89.6 |

F Limitations, Discussions, and Future Works

In our UniMatch, a confidence threshold is primarily set to suppress potentially incorrect pseudo labels. In some challenging scenarios, *e.g.*, COCO, however, we observe that around 20% pixels are discarded during the learning course. Therefore, how to make full use of these uncertain pixels and meantime avoid error accumulation will be a promising direction to further facilitate current semi-supervised algorithms. This may also enable our model to be more robust to different thresholds.

Moreover, our framework, along with its precedents, such as the FixMatch serials [55, 6, 5, 72, 61] and UDA [64], heavily relies on the pseudo labeling quality on unlabeled images. In case yielded pseudo labels are poor, it would be hard for our semi-supervised learner to mine meaningful knowledge from unlabeled images. Therefore, if the class distribution is highly imbalanced, the model will be gradually biased to majority classes during training and pseudo labeling, making the minority classes worse and worse. In addition, on common benchmarks, the domain gap between labeled and unlabeled images is rarely needed to be explicitly considered. However, in real worlds, the abundant unlabeled images can not share exactly the same domain as labeled images. The semi-supervised learner would benefit from more unlabeled images if it can well cope with domain shift.

Last but not least, existing academic settings in semi-supervised classification/segmentation/detection prefer to restricting labeled images to an extremely low proportion, *e.g.*, only providing 40 labels on the CIFAR-10 and 92 labeled images on the Pascal. Nevertheless, considering most real-world demands, it might be more practical to assume labeled images is in the tens of thousands, while unlabeled images are even more, might in millions. Actually, a prior work [80] already explored such a setting, but it is expected to be further improved, both in accuracy and training efficiency.

We leave the aforementioned four problems, namely 1) how to fully exploit uncertain pixels, 2) class imbalance in pseudo labeling, 3) domain shift in pseudo labeling, and 4) how to effectively benefit from millions of unlabeled samples together with considerable labeled ones, to our future works.

References

- [1] Inigo Alonso, Alberto Sabater, David Ferstl, Luis Montesano, and Ana C Murillo. Semi-supervised semantic segmentation with pixel-level contrastive learning from a class-wise memory bank. In *ICCV*, 2021. 3
- [2] Eric Arazo, Diego Ortego, Paul Albert, Noel E O’Connor, and Kevin McGuinness. Pseudo-labeling and confirmation bias in deep semi-supervised learning. In *IJCNN*, 2020. 2
- [3] Wele Gedara Chaminda Bandara and Vishal M Patel. Revisiting consistency regularization for semi-supervised change detection in remote sensing images. *arXiv:2204.08454*, 2022. 12
- [4] Olivier Bernard, Alain Lalande, Clement Zotti, Frederick Cervenansky, Xin Yang, Pheng-Ann Heng, Irem Cetin, Karim Lekadir, Oscar Camara, Miguel Angel Gonzalez Ballester, et al. Deep learning techniques for automatic mri cardiac multi-structures segmentation and diagnosis: is the problem solved? *TMI*, 2018. 12
- [5] David Berthelot, Nicholas Carlini, Ekin D Cubuk, Alex Kurakin, Kihyuk Sohn, Han Zhang, and Colin Raffel. Remixmatch: Semi-supervised learning with distribution alignment and augmentation anchoring. In *ICLR*, 2020. 3, 5, 13
- [6] David Berthelot, Nicholas Carlini, Ian Goodfellow, Nicolas Papernot, Avital Oliver, and Colin Raffel. Mixmatch: A holistic approach to semi-supervised learning. In *NeurIPS*, 2019. 3, 13
- [7] Avrim Blum and Tom Mitchell. Combining labeled and unlabeled data with co-training. In *COLT*, 1998. 3
- [8] Mathilde Caron, Ishan Misra, Julien Mairal, Priya Goyal, Piotr Bojanowski, and Armand Joulin. Unsupervised learning of visual features by contrasting cluster assignments. In *NeurIPS*, 2020. 5
- [9] Hao Chen and Zhenwei Shi. A spatial-temporal attention-based method and a new dataset for remote sensing image change detection. *RS*, 2020. 12
- [10] Liang-Chieh Chen, Yukun Zhu, George Papandreou, Florian Schroff, and Hartwig Adam. Encoder-decoder with atrous separable convolution for semantic image segmentation. In *ECCV*, 2018. 7
- [11] Ting Chen, Simon Kornblith, Mohammad Norouzi, and Geoffrey Hinton. A simple framework for contrastive learning of visual representations. In *ICML*, 2020. 2, 5
- [12] Xiaokang Chen, Yuhui Yuan, Gang Zeng, and Jingdong Wang. Semi-supervised semantic segmentation with cross pseudo supervision. In *CVPR*, 2021. 1, 2, 3, 6, 7, 12
- [13] Xinlei Chen and Kaiming He. Exploring simple siamese representation learning. In *CVPR*, 2021. 5
- [14] François Chollet. Xception: Deep learning with depthwise separable convolutions. In *CVPR*, 2017. 8
- [15] Marius Cordts, Mohamed Omran, Sebastian Ramos, Timo Rehfeld, Markus Enzweiler, Rodrigo Benenson, Uwe Franke, Stefan Roth, and Bernt Schiele. The cityscapes dataset for semantic urban scene understanding. In *CVPR*, 2016. 7
- [16] Terrance DeVries and Graham W Taylor. Improved regularization of convolutional neural networks with cutout. *arXiv:1708.04552*, 2017. 3, 7
- [17] Mark Everingham, SM Ali Eslami, Luc Van Gool, Christopher KI Williams, John Winn, and Andrew Zisserman. The pascal visual object classes challenge: A retrospective. *IJCV*, 2015. 7
- [18] Zhengyang Feng, Qianyu Zhou, Qiqi Gu, Xin Tan, Guangliang Cheng, Xuequan Lu, Jianping Shi, and Lizhuang Ma. Dmt: Dynamic mutual training for semi-supervised learning. *PR*, 2022. 3

- [19] Geoff French, Timo Aila, Samuli Laine, Michal Mackiewicz, and Graham Finlayson. Semi-supervised semantic segmentation needs strong, high-dimensional perturbations. In *BMVC*, 2020. 1, 3, 4, 6
- [20] Chengyue Gong, Dilin Wang, and Qiang Liu. Alphamatch: Improving consistency for semi-supervised learning with alpha-divergence. In *CVPR*, 2021. 3
- [21] Ian J Goodfellow, Jean Pouget-Abadie, Mehdi Mirza, Bing Xu, David Warde-Farley, Sherjil Ozair, Aaron Courville, and Yoshua Bengio. Generative adversarial networks. In *NeurIPS*, 2014. 1, 3
- [22] Yves Grandvalet and Yoshua Bengio. Semi-supervised learning by entropy minimization. In *NeurIPS*, 2005. 3
- [23] Dayan Guan, Jiaxing Huang, Aoran Xiao, and Shijian Lu. Unbiased subclass regularization for semi-supervised semantic segmentation. In *CVPR*, 2022. 1, 3
- [24] Bharath Hariharan, Pablo Arbeláez, Lubomir Bourdev, Subhransu Maji, and Jitendra Malik. Semantic contours from inverse detectors. In *ICCV*, 2011. 7
- [25] Kaiming He, Haoqi Fan, Yuxin Wu, Saining Xie, and Ross Girshick. Momentum contrast for unsupervised visual representation learning. In *CVPR*, 2020. 2, 5
- [26] Kaiming He, Xiangyu Zhang, Shaoqing Ren, and Jian Sun. Deep residual learning for image recognition. In *CVPR*, 2016. 7
- [27] Ruifei He, Jihan Yang, and Xiaojuan Qi. Re-distributing biased pseudo labels for semi-supervised semantic segmentation: A baseline investigation. In *ICCV*, 2021. 1, 3
- [28] Hanzhe Hu, Fangyun Wei, Han Hu, Qiwei Ye, Jinshi Cui, and Liwei Wang. Semi-supervised semantic segmentation via adaptive equalization learning. In *NeurIPS*, 2021. 1, 3, 4, 7
- [29] Xinyue Huo, Lingxi Xie, Jianzhong He, Zijie Yang, and Qi Tian. Atso: Asynchronous teacher-student optimization for semi-supervised image segmentation. In *CVPR*, 2021. 1
- [30] Jisoo Jeong, Seungeui Lee, Jeessoo Kim, and Nojun Kwak. Consistency-based semi-supervised learning for object detection. In *NeurIPS*, 2019. 3
- [31] Shunping Ji, Shiqing Wei, and Meng Lu. Fully convolutional networks for multisource building extraction from an open aerial and satellite imagery data set. *TGRS*, 2018. 12
- [32] Zhanghan Ke, Kaican Li Di Qiu, Qiong Yan, and Rynson WH Lau. Guided collaborative training for pixel-wise semi-supervised learning. In *ECCV*, 2020. 3
- [33] Chia-Wen Kuo, Chih-Yao Ma, Jia-Bin Huang, and Zsolt Kira. Featmatch: Feature-based augmentation for semi-supervised learning. In *ECCV*, 2020. 2
- [34] Donghyeon Kwon and Suha Kwak. Semi-supervised semantic segmentation with error localization network. In *CVPR*, 2022. 3, 6, 7
- [35] Xin Lai, Zhuotao Tian, Li Jiang, Shu Liu, Hengshuang Zhao, Liwei Wang, and Jiaya Jia. Semi-supervised semantic segmentation with directional context-aware consistency. In *CVPR*, 2021. 3, 6, 7
- [36] Samuli Laine and Timo Aila. Temporal ensembling for semi-supervised learning. In *ICLR*, 2017. 3
- [37] Dong-Hyun Lee et al. Pseudo-label: The simple and efficient semi-supervised learning method for deep neural networks. In *ICML Workshop*, 2013. 3
- [38] Junnan Li, Caiming Xiong, and Steven CH Hoi. Comatch: Semi-supervised learning with contrastive graph regularization. In *ICCV*, 2021. 3
- [39] Tsung-Yi Lin, Michael Maire, Serge Belongie, James Hays, Pietro Perona, Deva Ramanan, Piotr Dollár, and C Lawrence Zitnick. Microsoft coco: Common objects in context. In *ECCV*, 2014. 7

- [40] Shikun Liu, Shuaifeng Zhi, Edward Johns, and Andrew J Davison. Bootstrapping semantic segmentation with regional contrast. In *ICLR*, 2022. 2, 3, 5, 6
- [41] Yen-Cheng Liu, Chih-Yao Ma, Zijian He, Chia-Wen Kuo, Kan Chen, Peizhao Zhang, Bichen Wu, Zsolt Kira, and Peter Vajda. Unbiased teacher for semi-supervised object detection. In *ICLR*, 2021. 1, 4
- [42] Yuyuan Liu, Yu Tian, Yuanhong Chen, Fengbei Liu, Vasileios Belagiannis, and Gustavo Carneiro. Perturbed and strict mean teachers for semi-supervised semantic segmentation. In *CVPR*, 2022. 2, 3, 5, 6, 7, 8
- [43] Jonathan Long, Evan Shelhamer, and Trevor Darrell. Fully convolutional networks for semantic segmentation. In *CVPR*, 2015. 1
- [44] Xiangde Luo, Minhao Hu, Tao Song, Guotai Wang, and Shaoting Zhang. Semi-supervised medical image segmentation via cross teaching between cnn and transformer. In *MIDL*, 2022. 12
- [45] Luke Melas-Kyriazi and Arjun K Manrai. Pixmatch: Unsupervised domain adaptation via pixelwise consistency training. In *CVPR*, 2021. 1, 4
- [46] Robert Mendel, Luis Antonio de Souza, David Rauber, João Paulo Papa, and Christoph Palm. Semi-supervised segmentation based on error-correcting supervision. In *ECCV*, 2020. 3
- [47] Sudhanshu Mittal, Maxim Tatarchenko, and Thomas Brox. Semi-supervised semantic segmentation with high-and low-level consistency. *TPAMI*, 2019. 1, 3, 12
- [48] Takeru Miyato, Shin-ichi Maeda, Masanori Koyama, and Shin Ishii. Virtual adversarial training: a regularization method for supervised and semi-supervised learning. *TPAMI*, 2018. 3, 9
- [49] Yassine Ouali, Céline Hudelot, and Myriam Tami. Semi-supervised semantic segmentation with cross-consistency training. In *CVPR*, 2020. 1, 3, 9, 12
- [50] Daifeng Peng, Lorenzo Bruzzone, Yongjun Zhang, Haiyan Guan, Haiyong Ding, and Xu Huang. Semicdnet: A semisupervised convolutional neural network for change detection in high resolution remote-sensing images. *TGRS*, 2020. 12
- [51] Hieu Pham, Zihang Dai, Qizhe Xie, and Quoc V Le. Meta pseudo labels. In *CVPR*, 2021. 3
- [52] Siyuan Qiao, Wei Shen, Zhishuai Zhang, Bo Wang, and Alan Yuille. Deep co-training for semi-supervised image recognition. In *ECCV*, 2018. 3
- [53] Chuck Rosenberg, Martial Hebert, and Henry Schneiderman. Semi-supervised self-training of object detection models. In *WACV/MOTION*, 2005. 3
- [54] Mehdi Sajjadi, Mehran Javanmardi, and Tolga Tasdizen. Regularization with stochastic transformations and perturbations for deep semi-supervised learning. In *NeurIPS*, 2016. 3
- [55] Kihyuk Sohn, David Berthelot, Chun-Liang Li, Zizhao Zhang, Nicholas Carlini, Ekin D Cubuk, Alex Kurakin, Han Zhang, and Colin Raffel. Fixmatch: Simplifying semi-supervised learning with consistency and confidence. In *NeurIPS*, 2020. 1, 3, 10, 13
- [56] Nasim Souly, Concetto Spampinato, and Mubarak Shah. Semi supervised semantic segmentation using generative adversarial network. In *ICCV*, 2017. 1, 3
- [57] Yihe Tang, Weifeng Chen, Yijun Luo, and Yuting Zhang. Humble teachers teach better students for semi-supervised object detection. In *CVPR*, 2021. 1, 4
- [58] Antti Tarvainen and Harri Valpola. Mean teachers are better role models: Weight-averaged consistency targets improve semi-supervised deep learning results. In *NeurIPS*, 2017. 3
- [59] Aaron Van den Oord, Yazhe Li, and Oriol Vinyals. Representation learning with contrastive predictive coding. *arXiv:1807.03748*, 2018. 5

- [60] Tuan-Hung Vu, Himalaya Jain, Maxime Bucher, Matthieu Cord, and Patrick Pérez. Advent: Adversarial entropy minimization for domain adaptation in semantic segmentation. In *CVPR*, 2019. 12
- [61] Yidong Wang, Hao Chen, Qiang Heng, Wenxin Hou, Marios Savvides, Takahiro Shinozaki, Bhiksha Raj, Zhen Wu, and Jindong Wang. Freematch: Self-adaptive thresholding for semi-supervised learning. *arXiv:2205.07246*, 2022. 3, 13
- [62] Yuchao Wang, Haochen Wang, Yujun Shen, Jingjing Fei, Wei Li, Guoqiang Jin, Liwei Wu, Rui Zhao, and Xinyi Le. Semi-supervised semantic segmentation using unreliable pseudo-labels. In *CVPR*, 2022. 1, 2, 3, 5, 6, 7
- [63] Junfei Xiao, Longlong Jing, Lin Zhang, Ju He, Qi She, Zongwei Zhou, Alan Yuille, and Yingwei Li. Learning from temporal gradient for semi-supervised action recognition. In *CVPR*, 2022. 1, 4
- [64] Qizhe Xie, Zihang Dai, Eduard Hovy, Minh-Thang Luong, and Quoc V Le. Unsupervised data augmentation for consistency training. In *NeurIPS*, 2020. 3, 13
- [65] Qizhe Xie, Minh-Thang Luong, Eduard Hovy, and Quoc V Le. Self-training with noisy student improves imagenet classification. In *CVPR*, 2020. 3
- [66] Mengde Xu, Zheng Zhang, Han Hu, Jianfeng Wang, Lijuan Wang, Fangyun Wei, Xiang Bai, and Zicheng Liu. End-to-end semi-supervised object detection with soft teacher. In *ICCV*, 2021. 1, 4
- [67] Yinghao Xu, Fangyun Wei, Xiao Sun, Ceyuan Yang, Yujun Shen, Bo Dai, Bolei Zhou, and Stephen Lin. Cross-model pseudo-labeling for semi-supervised action recognition. In *CVPR*, 2022. 1, 4
- [68] Lihe Yang, Wei Zhuo, Lei Qi, Yinghuan Shi, and Yang Gao. St++: Make self-training work better for semi-supervised semantic segmentation. In *CVPR*, 2022. 1, 2, 3, 6, 7
- [69] Lequan Yu, Shujun Wang, Xiaomeng Li, Chi-Wing Fu, and Pheng-Ann Heng. Uncertainty-aware self-ensembling model for semi-supervised 3d left atrium segmentation. In *MICCAI*, 2019. 12
- [70] Jianlong Yuan, Yifan Liu, Chunhua Shen, Zhibin Wang, and Hao Li. A simple baseline for semi-supervised semantic segmentation with strong data augmentation. In *ICCV*, 2021. 1, 3
- [71] Sangdoon Yun, Dongyoon Han, Seong Joon Oh, Sanghyuk Chun, Junsuk Choe, and Youngjoon Yoo. Cutmix: Regularization strategy to train strong classifiers with localizable features. In *ICCV*, 2019. 2, 3, 7
- [72] Bowen Zhang, Yidong Wang, Wenxin Hou, Hao Wu, Jindong Wang, Manabu Okumura, and Takahiro Shinozaki. Flexmatch: Boosting semi-supervised learning with curriculum pseudo labeling. In *NeurIPS*, 2021. 3, 13
- [73] Hang Zhang, Kristin Dana, Jianping Shi, Zhongyue Zhang, Xiaogang Wang, Amrith Tyagi, and Amit Agrawal. Context encoding for semantic segmentation. In *CVPR*, 2018. 1
- [74] Jianrong Zhang, Tianyi Wu, Chuanghao Ding, Hongwei Zhao, and Guodong Guo. Region-level contrastive and consistency learning for semi-supervised semantic segmentation. In *IJCAI*, 2022. 3
- [75] Pan Zhang, Bo Zhang, Ting Zhang, Dong Chen, and Fang Wen. Robust mutual learning for semi-supervised semantic segmentation. *arXiv:2106.00609*, 2021. 3
- [76] Ying Zhang, Tao Xiang, Timothy M Hospedales, and Huchuan Lu. Deep mutual learning. In *CVPR*, 2018. 3
- [77] Hengshuang Zhao, Jianping Shi, Xiaojuan Qi, Xiaogang Wang, and Jiaya Jia. Pyramid scene parsing network. In *CVPR*, 2017. 1

- [78] Yuanyi Zhong, Bodi Yuan, Hong Wu, Zhiqiang Yuan, Jian Peng, and Yu-Xiong Wang. Pixel contrastive-consistent semi-supervised semantic segmentation. In *ICCV*, 2021. 3, 6, 7, 8, 10
- [79] Yanning Zhou, Hang Xu, Wei Zhang, Bin Gao, and Pheng-Ann Heng. C3-semiseg: Contrastive semi-supervised segmentation via cross-set learning and dynamic class-balancing. In *ICCV*, 2021. 3
- [80] Barret Zoph, Golnaz Ghiasi, Tsung-Yi Lin, Yin Cui, Hanxiao Liu, Ekin D Cubuk, and Quoc V Le. Rethinking pre-training and self-training. In *NeurIPS*, 2020. 3, 13
- [81] Yuliang Zou, Zizhao Zhang, Han Zhang, Chun-Liang Li, Xiao Bian, Jia-Bin Huang, and Tomas Pfister. Pseudoseg: Designing pseudo labels for semantic segmentation. In *ICLR*, 2021. 1, 3, 4, 6, 7, 8, 10